

# Blue stars in M32

Eva Busekool,  
Supervisor: S.C. Trager

June 5, 2008

## **Abstract**

We made color-magnitude diagrams of M32 from images taken with the Hubble Space Telescope/Wide-Field Planetary Camera 2. A blue plume is discovered above the horizontal branch. It is not clear if these stars are originally from M32 or from M31. Through counting the stars in the blue plume in different positions, we have suggest that these stars come originally from M32. It is not clear whether these stars are blue stragglers or massive young stars.

# Contents

<b>1</b>	<b>Introduction</b>	<b>3</b>
<b>2</b>	<b>Data and reduction</b>	<b>4</b>
2.1	Data . . . . .	4
2.2	Reduction . . . . .	6
<b>3</b>	<b>Color-magnitude diagram</b>	<b>7</b>
<b>4</b>	<b>Distance</b>	<b>10</b>
<b>5</b>	<b>Isochrones</b>	<b>10</b>
<b>6</b>	<b>Counting</b>	<b>12</b>
<b>7</b>	<b>Results</b>	<b>17</b>
7.1	Counting . . . . .	17
7.2	Comparison with M31 . . . . .	18
<b>8</b>	<b>Discussion and Conclusion</b>	<b>19</b>
8.1	Discussion . . . . .	19
8.2	Conclusion . . . . .	19

# 1 Introduction

M32 is the nearest elliptical galaxy. It is a satellite of M31, Andromeda. The spectrum is identical to other faint ellipticals [3]. The major diameter is 8.7 arcsec and the minor diameter is 6.5 arcsec. The classification is cE2 (a compact elliptical galaxy of class E2) [14]. A compact elliptical galaxy has a high surface density with respect to the radius, and a truncated de Vaucouleurs profile [4] [5]. Most of these compact elliptical galaxies are very close to a large/massive galaxies. A couple of theories of how these galaxies get such a high surface density are related to the interaction with a large/massive galaxy [5]<sup>1</sup>. One theory is that in the beginning M32 was a 'normal' elliptical galaxy. Because of the closeness of M31 the outer part of M32 was stripped off by M31 [6]. The outer part contains mostly small stars. The most of the massive stars in the core are left. What is left after the stripping is a very luminous compact galaxy. Another theory is proposed by A. Burkert [7], compact ellipticals are formed through starburst and the subsequent violent collapse of a close massive galaxy. M32 is very close to M31, only 22 arc minutes. M32 is located superimposed the outskirts of the spiral arms of M31. M32 has a velocity of  $-200 \pm 6$  km/s [14]. M31 has a velocity of  $-300 \pm 4$  km/s [14]. M32 has a relative velocity of 100 km/s towards M31.

The dominant stellar population in M32 is an old stellar population. Most of the stars are low-mass stars, mainly because the high-mass stars already died and the low-mass stars survived. The mean age of the stars is 8.5 Gyr [3]. Integrated light studies of M32 found spectral lines which show evidence for a hot/young stellar population.

On the color-magnitude diagrams of M32 the Red-Giant Branch is very broad, the spread in color is very large. This kind of spread in color requires a range in metallicity [3]. Grillmair et al. [3] made a metallicity distribution of M32. This distribution is very smooth and strongly skewed towards metal-rich stars. The peak of the metallicity occurs at  $-0.2 < [\text{Fe}/\text{H}] < +0.01$ .

M32 has a central black hole of  $2.5 * 10^6 M_{\odot}$  [8]. This is very massive. Comparing to the Milky Way, with a black hole of  $2.6 * 10^6 M_{\odot}$ , and M31, with a black hole of  $4.5 * 10^7 M_{\odot}$ , M32 seems a bit small for such a big black hole. M32 was probably much larger in the past.

A group led by T.R. Lauer<sup>2</sup> acquired high resolution images of M32 with the Hubble Space Telescope Advanced Camera for Surveys/High Resolution Camera (HST ACS/HRC). The main goal was to get information about the star formation history of M32. Therefore it is necessary to obtain the Main-Sequence Turn-off point. This was never obtained before, because the resolution was not high enough. After reduction of the data, they had a color-magnitude diagram of M32. A blue plume was discovered above the MSTO point, which had never been published. It is not clear what these stars are or where they come from<sup>3</sup>. The goal of this project is to determine whether the stars in the blue plume come originally from M32 or from M31. M32 is situated close to M31's central region and is overlaid over the outskirts of the spiral arms of M31. It is possible that these stars from M31 are superimposed over the stars of M32. The stars

<sup>1</sup>other references are cited in that paper

<sup>2</sup>Members of the rest of the group are: C.J. Grillmair, W.L. Freedman, A. Dressler, K. Mighell, S.C. Trager and A. Monachesi

<sup>3</sup>This information is obtained by private communication

Table 1: Fields in M32 and properties

Position	RA (hh mm ss)	DEC (dd mm ss)
Position 1	00 42 58.8	+40 50 34.7
Position 2	00 43 25.28	+41 04 02.2
Position 3	00 43 07.85	+40 53 33
Position 4	00 43 16.9	+40 46 31.08
Position 5	00 43 50.8	+40 59 35.74
Position 6	00 43 09.32	+40 56 36.68
Position	no. images F606W	no. images F814
Position 1	8	4
Position 2	8	4
Position 3	4	3
Position 4	14	4
Position 5	12	6
Position 6	4	4
Position	total exposure time F606W (sec)	total exposure time F814W (sec)
Position 1	8800.00	4400.00
Position 2	8800.00	4400.00
Position 3	1700.00	1100.00
Position 4	34700.00	10000.00
Position 5	29700.00	15000.00
Position 6	1400.00	1220.00

in the blue plume may come originally from M31 or may come from M32.

## 2 Data and reduction

### 2.1 Data

We use observations made with the Hubble Space Telescope/Wide-Field Planetary Camera 2 (HST/WFPC2). These images were obtained from the ESO/ST-ECF Science Archive [12]. The fields are taken at different positions in M32. Each field has several images taken with the F606W and F814W filter. The size of each field is a 150" x 150" square with one smaller quadrant (32" x 32") (the different quadrant are defined by PC (32" x 32"), WF2, WF3, and WF4) [12]. Properties of these fields are shown in Table 1. Further information about proposal IDs is in Appendix A.

We show in Figure 1 the positions with respect to the core of M32. The images are already calibrated using the standard pipeline data processing. This calibration is designed to remove most of the known instrumental signatures. The calibration consists of a determination of the global bias level, subtracting of the bias and dark, and applying a flat field frame. Each image is now part of a dataset, containing a calibrated image file, a calibrated image data quality file, a file with information about which images have which filter and the shift per image, and some other files, which we did not use.

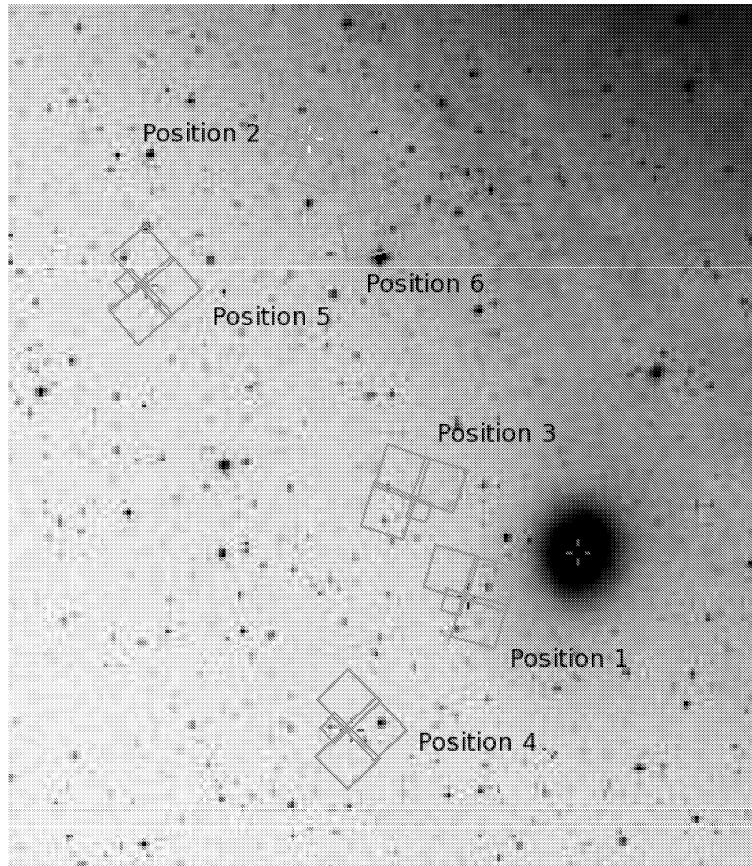


Figure 1: M32 with the fields

## 2.2 Reduction

We use HSTphot [13] for the photometry of the images, a photometry package specialised for HST/WFPC2 data. For the reduction of the data we use the following tasks: ‘mask’, ‘getsky’, ‘crmask’, and ‘hotpixels’. ‘Mask’ masks bad pixels and other image defects with the use of the image data quality file. The program sets bad pixels to a bad data value (usually  $-100$ ). The masked pixels are not used by the other programs. ‘Getsky’ creates a sky-image. This sky-image is used during the final routine ‘hstphot’, the real image is substrated by the sky-image. The sky-image is made by taking all pixels around one pixel and using a robust mean estimator for determining the sky value of that pixel. This routine can be done a lot faster, if a very precise calculation is not needed. A second call of ‘Getsky’ takes pixels at selected values and interpolates to compute a sky-image. This option is recommended if the sky option within ‘hstphot’ is used. We are going to use the sky option while running hstphot, so this abbreviated routine is good enough for our images. ‘Crmask’ removes cosmic rays. At least two images are required for this procedure. The images don not have to be perfectly aligned, as a shift between the first and following images can be given. The so called asn-file gives the shift from each images with respect to the first image. These shifts are the same as those we calculated, so we can use these shifts. According to the HSTphot User’s Guide the routine can even handle images from different filters. This is not our conclusion. If we put images taken with different filters together through the routine, ‘crmask’ masks all the centres of the stars. It is very difficult to photometer the image when it does not contain stars. If we put only the images of the same filter together through the routine, the images come out without cosmic rays and with stars. For one position there was a problem. For position 6 (see Table 1) the shifts between the images were too large to use the routine crmask. Without this routine it is impossible to photometer the images. So we leave this position out of this project. The last routine for the reduction is ‘hotpixels’. ‘Hotpixels’ masks hot pixels, which are equally high in all images. The hot pixels are also given the bad pixel value ( $-100$ ).

After this preprocessing we use the routine ‘hstphot’ photometer the images. All images (also from different filters) at one position ran together to determine the best photometry. The shift of each image with respect to the reference image is therefore required. With running multiple images together it is easier to compensate for bad pixels or cosmic rays. Cosmic rays mostly occur on only one image. Also a more stable photon count is obtained by reducing the number of free parameters. Counting the photons, X, and Y apart in each image, the number of free parameters is  $3 \times N_{images}$ . With determining the global X and Y position and counts in each image, the number of free parameters is now reduced to  $2 + N_{images}$ . Now a more stable photon count is obtained, stars and non-stellar object are easier to detect.

The output of hstphot is a large table. Each line contains information about an object, which might be a star. From each line, the first three columns contain information about the chip value and the x and y position. The next six columns contain information about  $\chi$ , signal-to-noise ratio, sharpness, roundness, major axis, and object type. Some of these are good qualities to distinguish if the object indeed is a star.  $\chi$  gives the quality of the fit. The value of  $\chi$  should be less then 1.5, but values up to 2.5 are also reasonable. The second useful

Table 2: Number of stars

Position	no. of stars
Position 1	48534
Position 2	49509
Position 3	39815
Position 4	40951
Position 5	43278

value is the sharpness. If an object is too sharp ( $> 0.5$ ) it might be a cosmic ray and if it is too broad ( $< -0.5$ ) it might be a cluster or a galaxy. The last, very important, value for determining whether the object is indeed a star is object type. This is 1 for good star. The other possibilities are: possible unresolved binary (2), bad star (3), single-pixel cosmic ray or hot pixel (4), and extended object (5). After this comes the blocks of the photometry. The first two blocks of ten columns give the average values per filter. After this, blocks with the values per image are given. Each block contains the same values: counts, background, flight system magnitude, standard magnitude, magnitude uncertainty,  $\chi$ , signal-to-noise, sharpness, roundness and crowding. Flight system magnitude is the magnitude from the filters from the HST/WFPC2 (F606W and F814W). The standard magnitude is the magnitude transformed to the Johnson system (V and I). We choose to take the standard magnitude, because it is easier with respect to further applications (isochrones).

For this project we want the average standard magnitude in both filters of the ‘real’ stars. So we first select good values of  $\chi$ , sharpness, and object type. If these values are correct, we print out the values of the average standard magnitude in both filters. We use the program awk to do this.

### 3 Color-magnitude diagram

The results of the number of ‘good’ stars after the selection is shown in Table 4. This is an adequate amount to construct a color-magnitude diagram (CMD). We make two kinds of CMD’s,  $V - I$  vs.  $m_V$  and  $V - I$  vs.  $m_I$ . The CMDs are corrected for reddening and extinction. The formula for reddening is  $(V - I)_0 = (V - I) - (A_V - A_I)$ , and for extinction is  $m_{V/I,0} = m_{V/I} - A_{V/I}$ . The values of  $A_V$  and  $A_I$  are taken from the Galactic Extinction Calculator from the website of NED. The values are  $A_V = 0.206$  and  $A_I = 0.120$  respectively. The CMD’s are shown in Figure 2 – 6.

Almost all the stars are between  $(V - I) = -1$  and  $(V - I) = 5$ . The main feature in the CMDs is the Red Giant Branch (RGB) (between  $(V - I) = 0$  and  $(V - I) = 1.5$ ). The Tip of the Red Giant Branch (TRGB) is very well visible. We see another feature, the Horizontal Branch (HB) at  $(V - I) = 0$ . We also see a blue plume at  $(V - I) = 0$ , above the HB. The blue plume looks different at every CMD.

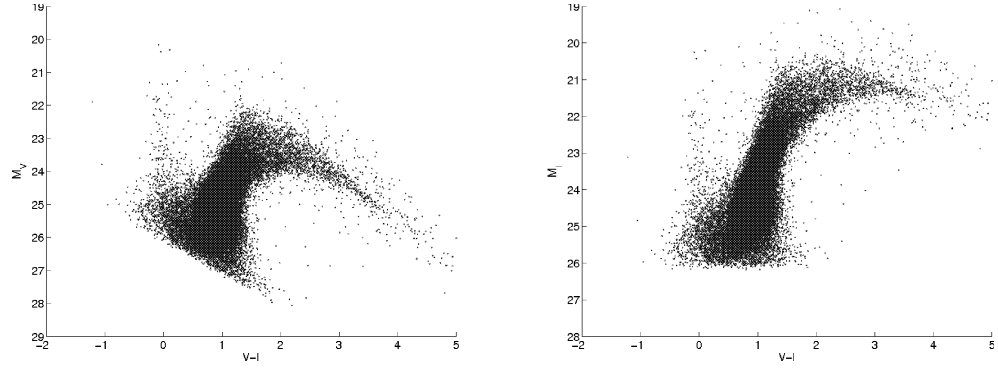


Figure 2: CMDs of position 1, number of stars is 48534,  $(V-I)$  vs.  $M_V$  is on the left and  $(V-I)$  vs.  $M_I$  is on the right. The main features are the Red Giant Branch, the Tip of the Red Giant Branch and the Horizontal Branch. Above the HB the blue plume is situated.

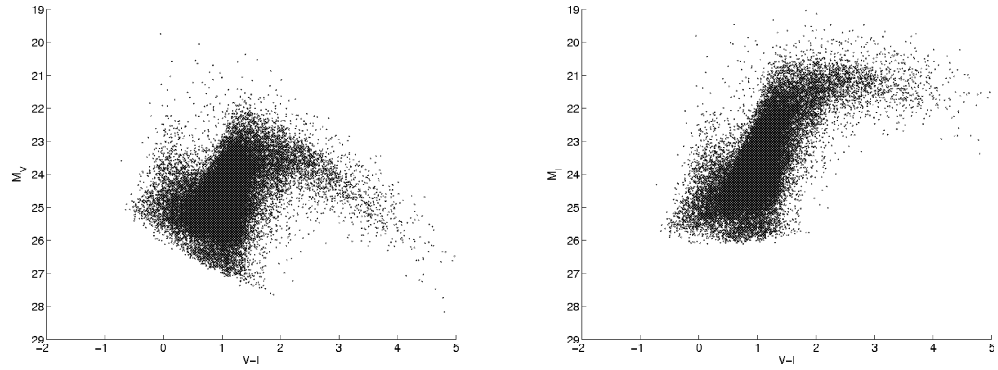


Figure 3: CMDs for position 2, number of stars is 49509. Other features as in Figure 2.



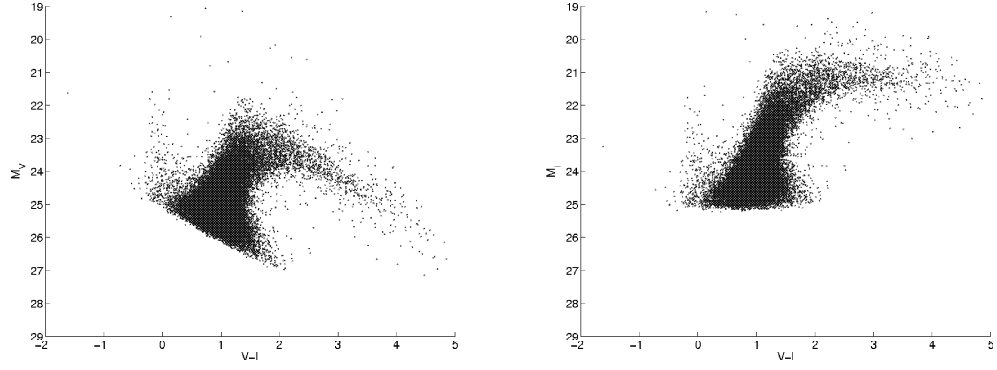


Figure 4: CMDs for position 3, number of stars is 39815. Other features as in Figure 2.

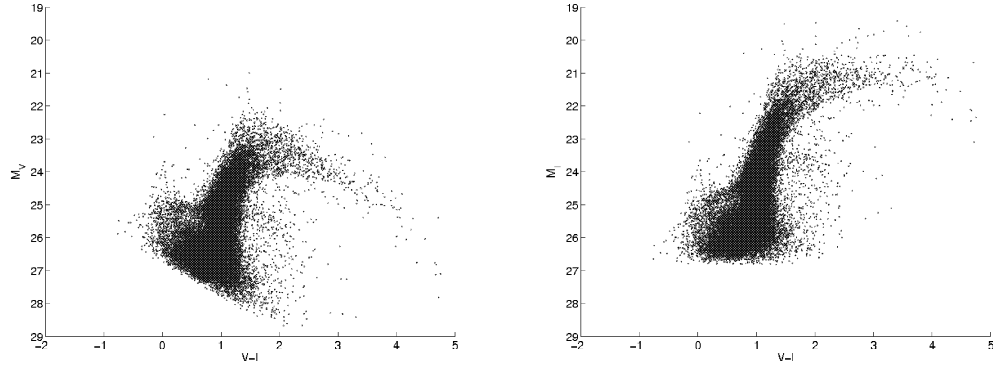


Figure 5: CMDs for position 4, number of stars is 40951. Other features as in Figure 2.

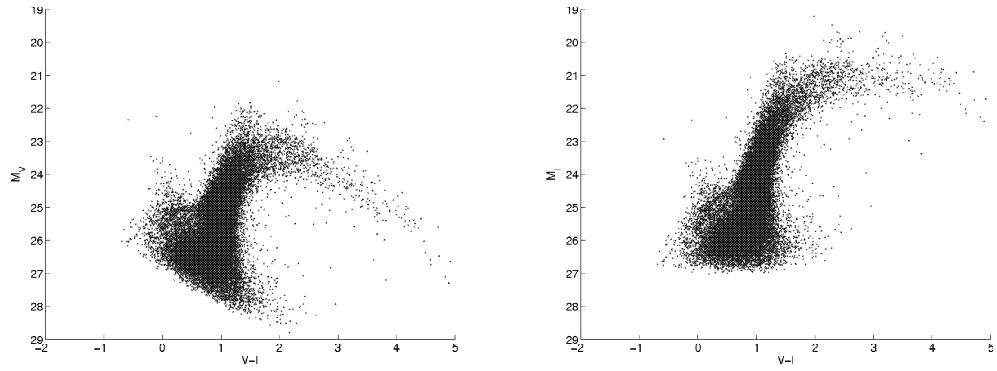


Figure 6: CMDs for position 5, number of stars is 43278. Other features as in Figure 2.

## 4 Distance

We need the distance modulus for the plotting of the isochrones (done in next section). We use the bolometric luminosity of the Tip of the Red Giant Branch (TRGB). The TRGB is very well visible on the CMDs. When the chemical composition of the star is fixed the mass of the helium (He) core at the He flash determines the bolometric luminosity of the TRGB. A He flash occurs when the He core reaches a mass of  $M_{cHe} \approx (0.48 - 0.50)M_{\odot}$ . This is approximately the same mass for low mass stars. The bolometric luminosity of the TRGB is approximately the same for ages between 4 and 14 Gyr. In the I-band the dependence of  $M_{bol}^{TRGB}$  on the metallicity is minimized. So  $M_I^{TRGB}$  is a good distance indicator for old ( $> 4$  Gyr), metal-poor single stellar population. M32 is not metal-poor. According to Grillmair et al. the peak of the metallicity is at  $-0.2 < [Fe/H] < +0.01$  and the low metallicity tail extends to  $[Fe/H] \approx -1.5$ . *And the method could be applied to systems as long as the galaxies show an appreciable population of low-mass, resolved, red giant branch stars with  $[Fe/H] < -0.7$  dex* [3]. The low-mass RGB stars with low metallicity in M32 are very faint, a magnitude fainter than the other, not-metal-poor, stars. For M32 the  $M_I = -3.7$  [3], the difference from  $M_I = -4$  is negligible. The age of M32 is approximately 8 Gyrs. We can use this method for distance determination. The formula for calculating the distance modulus from the TRGB is:

$$(m - M)_0 = I_{0,TRGB} - M_I^{TRGB} \quad (1)$$

$(m - M)_0$  is the distance modulus we want.  $I_{0,TRGB} = m_I - A_I$ .  $m_I$  is determined by making an histogram of the number of stars at different magnitudes. From the CMD we obtain an approximate value of the magnitude of the TRGB. We look at the histogram at the approximate value and search for a clear discontinuity. The discontinuity is at the value of  $m_I$  is  $20.6 \pm 0.1$ .  $A_I = 0.120$ .  $M_I^{TRGB} = -4$  for stars with  $[Fe/H] < 0.7$ . After a short calculation we find the distance modulus:  $(m - M)_0 = 24.48 \pm 0.1$ . This outcome seems to agree with Grillmair et al. [3], which found a distance modulus of  $24.43 \pm 0.09$ . The outcome also agree with Jensen et al. [15], they found an distance modulus of  $24.39 \pm 0.08$ . A different method was used, infrared surface brightness fluctuations.

## 5 Isochrones

An isochrone is a theoretical CMD for a single stellar population (SSP). The stars on an isochrone have the same age and metallicity, but different masses. There are different sets of isochrones. The Basti and Yonsei-Yale isochrones are used for this project. The goal of using isochrones is to make a rough estimate about the age and metallicity of the blue plume. The Yonsei-Yale isochrones are downloaded from [16]. This contains a program which interpolates the isochrones using an input file. Experimentation with the parameters is possible without downloading all the isochrones one by one. Eventually we came to the ages and other parameters seen in Table 5. Plots of the CMDs with the Yonsei-Yale isochrones are in Figure 7 – 11. The isochrones seem to fit well. We downloaded the Basti isochrones [17] with (almost) the same age and metallicity than the Yonsei-Yale isochrones. The Basti isochrones have the parameters seen in Table 6. The diagrams with the CMDs and the Basti isochrones are in

Table 3: Ages en other parameters of YY isochrones

Age (Gyr)						
0.15	0.20	0.25	0.30	0.35	0.40	0.45
[Fe/H]	[Alpha/H]	Z		Y	OS	l/Hp
0.00	0.00	0.018120	0.266239	0.20	1.743201	

Table 4: Ages and other parameters of the Basti isochrones

Age (Gyr)							
0.03	0.04	0.05	0.06	0.07	0.08	0.09	0.10
0.15	0.20	0.25	0.30	0.35	0.40	0.45	
[Fe/H]	[M/H]	Z		Y			
0.06	0.58	0.0198	0.273				

Figure 12 – 16. Also these isochrones seem to fit well. Even the very young isochrones fit with the stars in the blue plume.

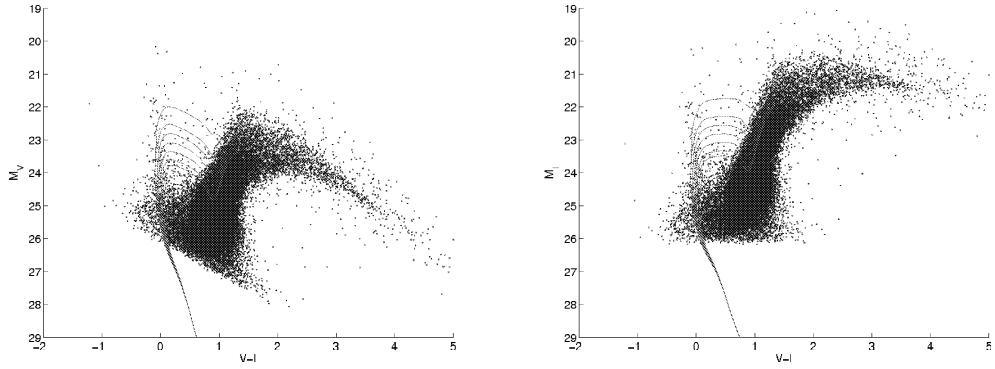


Figure 7: A CMD of position 1 as in Figure 2, with Yonsei-Yale isochrones. The ages are 0.15, 0.20, 0.25, 0.30, 0.35, 0.40 and 0.45 Gyr. The other parameters are:  $[\text{Fe}/\text{H}] = 0.00$ ,  $[\text{Alpha}/\text{H}] = 0.00$ ,  $Z = 0.018120$ ,  $Y = 0.266239$ ,  $\text{OS} = 0.20$  and  $l/\text{Hp} = 1.743201$ .

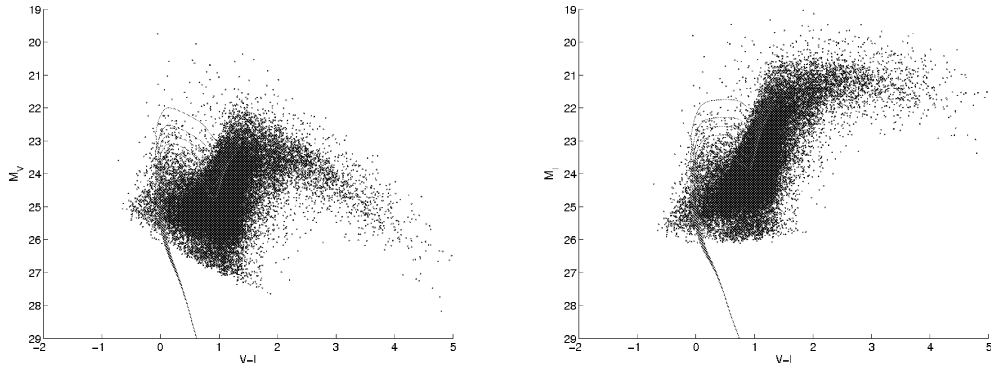


Figure 8: A CMD of position 2, as seen in Figure 7.

## 6 Counting

Each CMD at a different position has a different blue plume. Some positions seems to have more stars in the blue plume than other positions. We are going to count the stars in the blue plume at each position to see if this is the case. We have two ways to count the stars in the blue plume. The first way is to define a box around the blue plume and count all the stars in the box. The second way is to count the stars between the isochrones.

A box is defined in such way that only the stars in the blue plume are inside. Each CMD is different. For each CMD a different box is defined to avoid counting stars from the RGB and HB. This means that the box is not a rectangle. One side, along the RGB, is diagonal. An example of position 1 is shown in Figure 17. The boundaries of the boxes of all positions are given in appendix

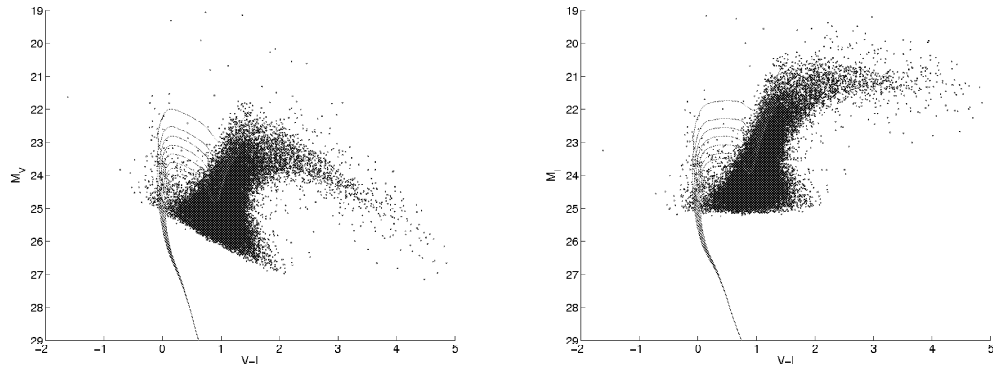


Figure 9: A CMD of position 3, as seen in Figure 7.

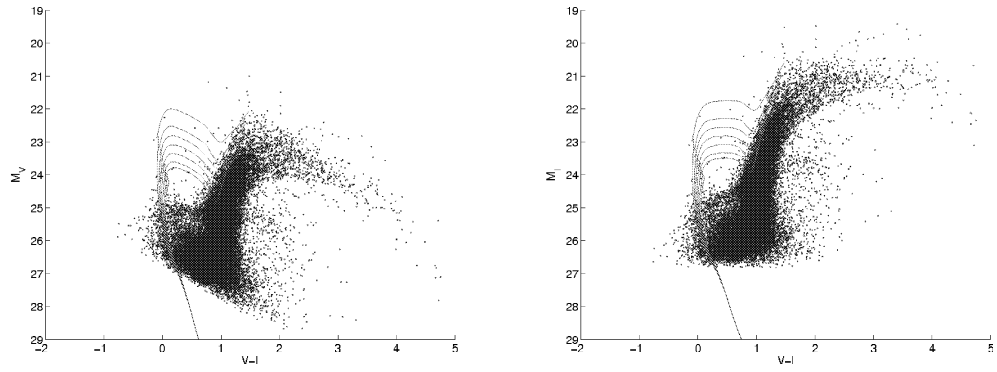


Figure 10: A CMD of position 4, as seen in Figure 7.

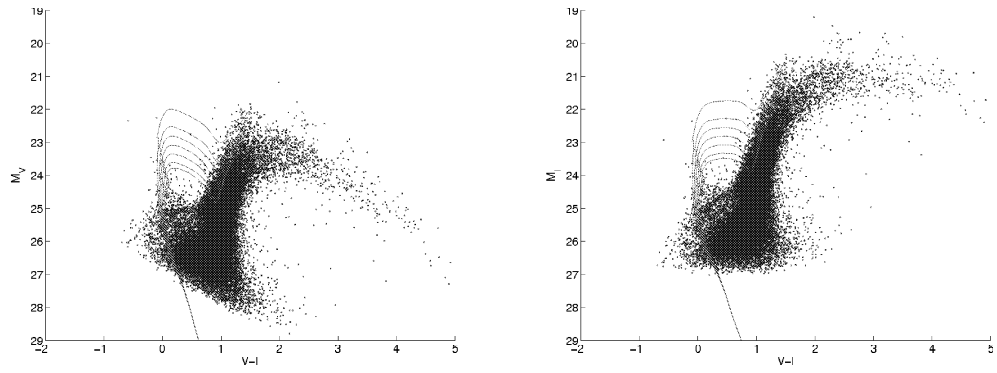


Figure 11: A CMD of position 5, as seen in Figure 7.

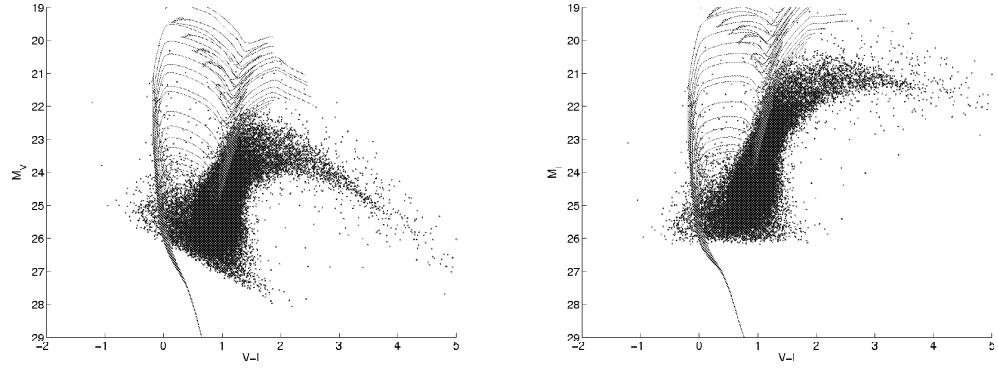


Figure 12: A CMD of position 1 as in Figure 2, with Basti isochrones. The ages are 0.03, 0.04, 0.05, 0.06, 0.07, 0.08, 0.09, 0.10, 0.15, 0.20, 0.25, 0.30, 0.35, 0.40 and 0.45 Gyr. The other parameters are:  $[\text{Fe}/\text{H}] = 0.06$ ,  $[\text{M}/\text{H}] = 0.58$ ,  $Z = 0.0198$  and  $Y = 0.273$

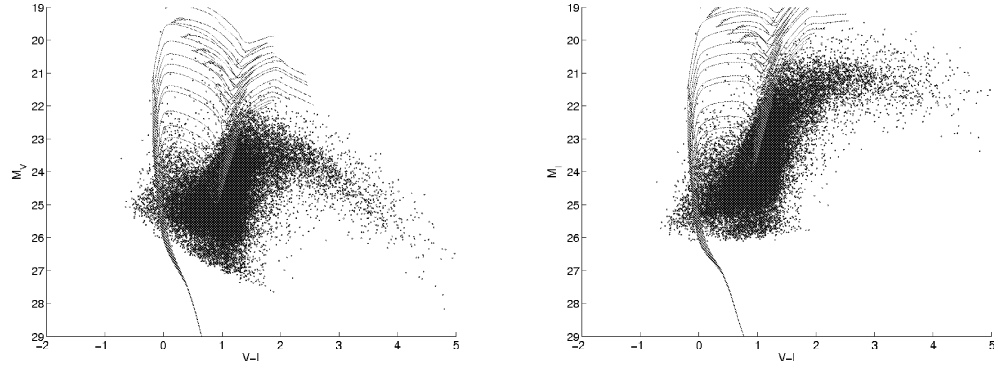


Figure 13: A CMD of position 2, as seen in Figure 12.

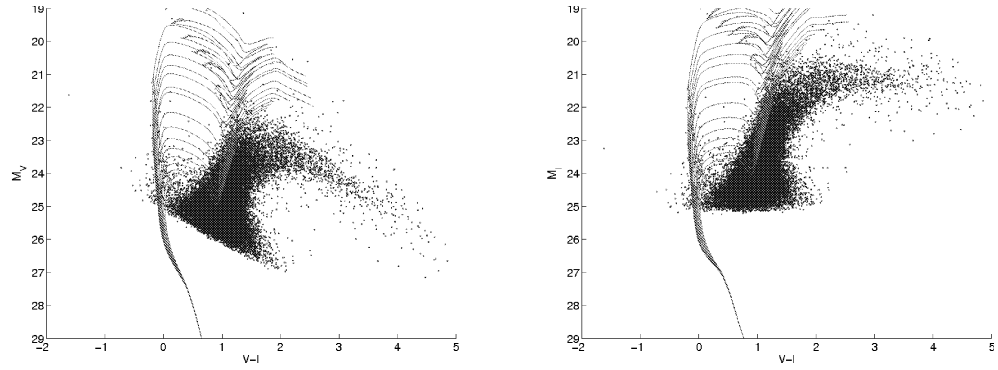


Figure 14: A CMD of position 3, as seen in Figure 12.

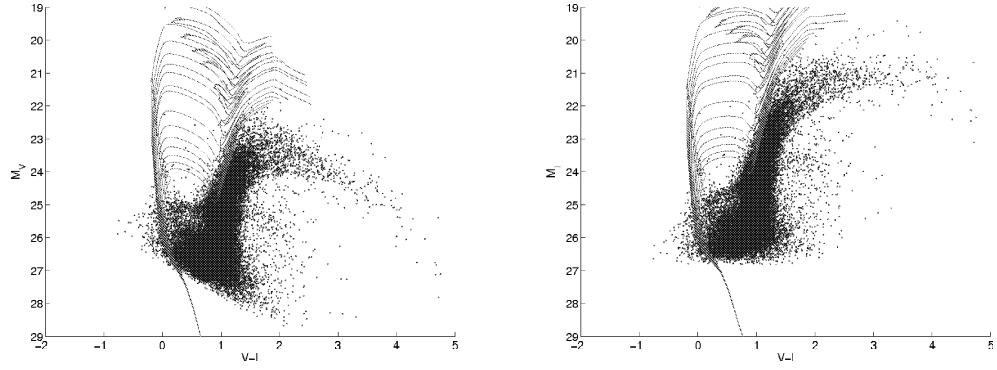


Figure 15: A CMD of position 4, as seen in Figure 12.

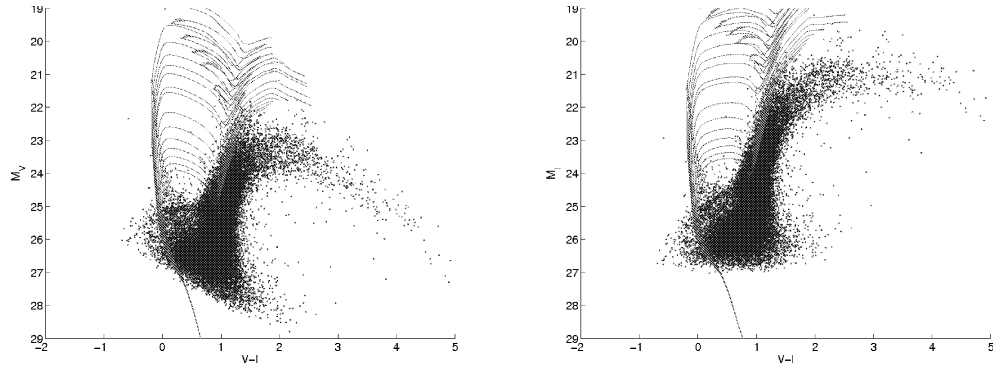


Figure 16: A CMD of position 5, as seen in Figure 12.

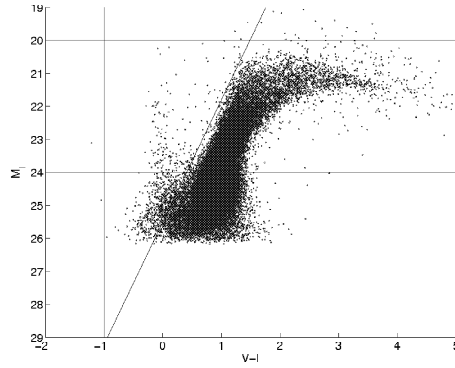


Figure 17: A CMD of position 1 with an example of a box in which the stars are counted.  $(V - I)_{min} = -1$ ,  $(V - I)_{max} = -3.7 * M_I + 25.5$ ,  $M_{I,min} = 20$ , and  $M_{I,max} = 24$

Table 5: Results of the counting in a box

	stars	%	stars	%
Position	V box		I box	
Position 1	192	0.3956	181	0.3729
Position 2	149	0.3010	140	0.2828
Position 3	117	0.2939	124	0.3114
Position 4	55	0.1343	41	0.1001
Position 5	55	0.1271	32	0.0739

Table 6: Counting between YY isochrones

Position	V yy isochrones		I yy isochrones	
Position 1	90	0.1854	92	0.1896
Position 2	50	0.1010	59	0.1192
Position 3	62	0.1557	68	0.1708
Position 4	20	0.0488	13	0.0317
Position 5	30	0.0693	17	0.0393

B. The results of the counting are shown in Table 7. The isochrones need some change before the counting. Counting between the whole isochrones means also counting stars in the HB and RGB. To solve this problem we only count between the part of the isochrones which fit the stars in the blue plume. A similar box is drawn (as seen in Figure 17) and only the part of the isochrones which fall in that box will remain. The boundaries of the boxes of all positions are given in appendix B. We count between these parts of the isochrones using the matlab program MDF.m [18]. The results of the counting between the Yonsei-Yale isochrones are in Table 6 and the results of the counting between the Basti isochrones are in Table 7.

The blue plume is very different at each position. To see if there is a correlation between the number of stars in the blue plume and the position of field with respect to the core of M32, we also determined the angular distance of each position to the core of M32. A program is written to do this. The results are shown in Table 8.

Table 7: Counting between the Basti isochrones

Position	V basti isochrones		I basti isochrones	
Position 1	169	0.3482	175	0.3606
Position 2	110	0.2222	107	0.2161
Position 3	116	0.2913	112	0.2813
Position 4	41	0.1001	36	0.0879
Position 5	51	0.1178	29	0.0670



Table 8: Angular distance

Position	RA	DEC	angular distance (deg)
Core M32	00 42 41.9	+40 51 57.2	0.0000
Position 1	00 42 58.8	+40 50 34.7	0.0742
Position 2	00 43 25.28	+41 04 02.2	0.2497
Position 3	00 43 07.85	+40 53 33	0.0622
Position 4	00 43 16.9	+40 46 31.08	0.1013
Position 5	00 43 50.8	+40 59 35.74	0.2630

Table 9: Summary of the counting in a box

Position	angular distance (deg)	average stars	%
Position 1	0.0742	186	0.3840
Position 2	0.2497	145	0.2919
Position 3	0.0622	121	0.3027
Position 4	0.1013	48	0.1172
Position 5	0.2630	44	0.1005

## 7 Results

### 7.1 Counting

The main question of this project whether the stars in the blue plume come originally from M32 or M31. A summary of the counting in a box is seen in Table 9. Positions 1 and 3 are the closest to the core of M32. According to the counting these positions contain many stars in the blue plume. Positions 4 and 5 are further away and contain fewer stars in the blue plume. Position 2 is the one with the largest angular diameter away from the core of M32. This position contains according to the counting many stars in the blue plume. Comparing the CMD of this position with the CMDs of the other positions a difference is visible. The CMD of position 2 has a broader RGB and more stars outside the 'regular path'. Position 2 is the closest to the core of M31. If there are more stars outside the 'regular path', automatically more stars are counted. Our conclusion is that this CMD is too different with respect to the others. The counting of the stars is not trustable any more. We leave this position out of our conclusion.

On the other positions we performed a chi-squared test on the number of stars in each position. The null-hypothesis is that each position contains an equally amount of stars (average number of stars  $H_0 = 99.75$ ). The outcome of the chi-squared test is 11.71. In table A2.6 of [19] is seen that a value of 9.84 is needed for a  $P = 0.02$ . So the null-hypothesis is rejected, each position does not contain an equally amount of stars. Position 1 and 3 contain the most stars in the blue plume, also in percentage. These positions are very close to the core of M32 in comparison to position 4 and 5. The stars occur mostly close to the core of M32. Therefore we suggest that the stars in the blue plume belong to M32.

A summary of the counting between the Yonsei-Yale isochrones is in table 10. The number of stars between the isochrones are less than the number of stars counted in a box. But the relative differences between the positions are almost

Table 10: Summary of counting yy isochrones

Position	angular distance (deg)	average stars	%
Position 1	0.0742	91	0.1875
Position 2	0.2497	55	0.1101
Position 3	0.0622	65	0.1633
Position 4	0.1013	17	0.0403
Position 5	0.2630	24	0.0543

Table 11: Summary of the counting between the Basti isochrones

Position	angular distance (deg)	average stars	%
Position 1	0.0742	173	0.3546
Position 2	0.2497	109	0.2192
Position 3	0.0622	114	0.2863
Position 4	0.1013	39	0.1880
Position 5	0.2630	40	0.0924

the same. Our conclusion still stands. Approximately half of the blue stars have ages between 0.15 and 0.45 Gyr and  $[Fe/H] \approx 0.00$ .

A summary of the counting between the Basti isochrones is in table 11. Counting between this set of isochrones gives more stars. The numbers of stars are almost the same as the numbers of stars from the counting in a box. Our conclusion is still the same. Almost all the stars are between the isochrones of 0.03 and 0.45 Gyrs. Nearly all the stars have ages between 0.03 and 0.45 Gyrs and  $[Fe/H] \approx 0.06$ .

## 7.2 Comparison with M31

Another way to estimate whether the stars in the blue plume come originally from M32 or from M31, is to look at CMDs from M31 and see if we can find a similar populations of stars. Brown et al. [20] made CMDs of M31. Brown et al. have found a population of plume of blue, young, and metal-rich stars in the disk of M31. These stars are situated above the Horizontal Branch (HB). The colorindex is  $(V - I) \approx -1$ . The stars in the blue plume we found are also situated above the HB, but these stars are redder. The colorindex is  $(V - I) \approx 0$ . This could be an effect of the use of different magnitude. Brown et al. use the flight system magnitude and in this project we use the standard magnitude. To test whether the stars of the different galaxies are the same stars, new CMDs of M32 are made with the flight system magnitude. At the new CMDs the blue plume is still at  $(V - I) \approx 0$ . The stars described by Brown et al. are not the same stars in our blue plume. The conclusion is that, also from the paper research, the stars in the blue plume come originally from M32.

## 8 Discussion and Conclusion

### 8.1 Discussion

In our color-magnitude diagrams of M32 a blue plume has been discovered. This blue plume is situated above the main sequence (MS) turn-off point. It is not clear what these stars are. The stars are situated outside the evolutionary track of a single stellar population. An evolutionary track is the change in location on the Hertzsprung-Russel diagram or CMD of a single star. A star evolves in time, so the place on a CMD changes with time. Stars with the same mass follow the same evolutionary track. There are two possibilities as to what these stars could be: blue stragglers or young massive stars. Blue stragglers are stars situated above and blue-ward of the MS turn-off. These stars seem to have somehow be refuelled with hydrogen. Blue stragglers maybe formed by evolution of primordial binairies or by collisions of two or more stars [9]. Both are likely to occur. Primordial binairies must evolve quietly without collisions to start the mass-transfer phase. Therefore the density must not have been too high. For blue stragglers formed from collisions the density must be sufficiently high to have a short collision time-scale. Globular clusters have sufficient high density to contain collisional blue stragglers.

There are a couple of differences between blue stragglers and young massive stars. A difference is that young stars follow an evolutionary track on the Hertzsprung-Russel (HR) diagram. So after being on the MS and MS turn-off they go up to the Sub Giant Branch (SGB) (which lead to the Red-Giant Branch (RGB)). If stars are detected on the SGB, then the stars in the blue plume are young stars. The stars in the blue plume are more massive than the dominant MSTO stellar population. A problem with detecting stars on the SGB is that massive stars spend very little time on the SGB. So observing them is very hard. In CMD of massive stars seems to be a discontinuity in the diagram, this is called the Hertzsprung gap. On the CMDs made with this project, no stars are detected on the SGB. No conclusion can be given whether these stars are young/hot stars or blue stragglers.

### 8.2 Conclusion

We wanted to determine whether stars in a blue plume above the Horizontal Branch of a color-magnitude diagram of M32 come originally from M32 or from M31. Therefore CMDs of different positions of M32 are made with data from the Hubble Space Telescope/Wild-Field Planetary Camera 2. To determine whether the stars in the blue plume are originally come from M32 or M31, we counted the stars in the blue plume in 2 different ways. The first method is counting the stars in a box drawn around these stars. The second way is to put isochrones on the blue plume and count stars between the isochrones. This is done for two sets of isochrones, Yonsei-Yale isochrones and Basti isochrones. All the methods count more stars for the positions close to the core of M32 than the positions further away from the core of M32. We also looked at CMDs of M31 to see if we could find such a blue plume. This is not the case. From the results of both countings and the lack of a blue plume in CMDs of M31, we suggest that the stars in the blue plume come originally from M32. Stars in this region of a CMD (above the HB) could be very young and hot stars

or blue stragglers. With the data we had it is not possible to determine if the stars in the blue plume or young/hot stars or blue stragglers. We determined that the stars in the blue plume come originally from M32, but it is not clear what kind of stars they are.

### Acknowledgements

I would like to thank my supervisor, S.C. Trager, for the help and support during this project and A. Monachesi for the information, which was usefull for the introduction.

## A

Table 12: Fields in M32: observers and proposal ID's

Position	Observer	Proposal ID
Position 1	Worthey	6664
Position 2	Worthey	6664
Position 3	Green	7566
Position 4	Mateo	9392
Position 5	Mateo	9392
Position 6	Worthey	7426

## B

Table 13: Boundaries of the box for the counting of the stars. These boundaries are the same for all positions:  $(V - I)_{min} = -1$ ,  $M_{I,min} = 20$ . The boundary of  $(V - I)_{max}$  is a formula, because the RGB is diagonal. The formula in the table is the following:  $M_{V/I} = a * (V - I) + b$ , a and b are constants(in the Table x is  $(V - I)$ ).

Position	formula for $(V - I)$ max	boundary for $M_{v/I}$ min
V box		
Position 1	-3.5x+26	24.5
Position 2	-3.5x+26	23.5
Position 3	-3.5x+26	24
Position 4	-3.5x+26.5	25
Position 5	-3.7x-26	25
V isochrones		
Position 1	-3.5x+26	24.5
Position 2	-3.5x+26	23
Position 3	-3.5x+25.5	24
Position 4	-3.5x+26.5	25
Position 5	-3.7x+26	25
I box		
Position 1	-3.7x+25.5	24
Position 2	-3.7x+25	23
Position 3	-3.7x+25.5	24
Position 4	-4.2x+26.5	24
Position 5	-4.4x+26.5	24
I isochrones		
Position 1	-3.7x+26	24
Position 2	-3.7x+25	23
Position 3	-3.7x+25.5	24
Position 4	-4.2x+26.5	24
Position 5	-4.4x+26.5	24

Table 14: Counting in a box

Position	$N_{starsinblueplume}$	$N_{RGBstars}$	$N_{starsinblueplume}/N_{RGBstars}$	angular distance (deg)
Position 3	111	18344	0.0061	0.0622
Position 1	145	19725	0.0074	0.0742
Position 4	16	8710	0.0018	0.1013
Position 2	489	25579	0.0191	0.2497
Position 5	24	10026	0.0024	0.2630

## C

A couple of days before the presentation we found out that the counting could be done better. The improvement is that the drawn box is the same for all position and that we calculate  $N_{blueplumestars}/N_{RGBstars}$  instead of  $N_{blueplumestars}/N_{restofthestars}$ . We now take the ratio above a certain magnitude. This is better, because the different positions have different depths. Now a better comparison can be made between the positions. The results of this counting are shown in Table 14. The results are sorted on angular distance.

## References

- [1] M. Salaris and S. Cassisi, Evolution of stars and stellar populations, John Wiley and Sons Ltd, 2005
- [2] M. Zelik and S.A. Gregory, Introductory astronomy and astrophysics, fourth edition, 1998
- [3] Grillmair et al.(1996), Astron. J., **112** (5)
- [4] J.-L. Nieto and P. Prugniel, Astron. Astrophys. 186, 30-38 (1987)
- [5] K.Bekki et al., ApJ, 557: L39-L42, 2001
- [6] S.M.Faber, ApJ, **179**: 423-426, 1973
- [7] A. Burkert, Mon. Not. R. Astron. Soc, **226**, 877-885 (1994)
- [8] Luis C. Ho et al., ApJ, **589**: 783-789, 2003
- [9] M. Mapelli et al. (2007), Mon. Not. R. Astron. Soc. **380**, 1127-1140
- [10] <http://seds.org/MESSIER/m/m032.html>
- [11] W. Baade, 1944ApJ, 100, 137B
- [12] <http://archive.eso.org/cms/>
- [13] <http://purcell.as.arizona.edu/hstphot/>
- [14] <http://nedwww.ipac.caltech.edu/forms/calculator.html>
- [15] J.B. Jensen et al., ApJ, **538**: 712-716, 2003
- [16] <http://www-astro.physics.ox.ac.uk/yi/yyiso.html>
- [17] <http://193.204.1.62/index.html>
- [18] A matlab program written by T.P.R. van der Laan
- [19] J.V. Wall and C.R. Jenkins, Practical statistics for astronomers, first published 2003
- [20] Brown et al.(2006), ApJS, **652**, 323-353